

## Optimizing structural topology patterns using regularization of Heaviside function

Dongkyu Lee<sup>1a</sup> and Soomi Shin<sup>\*2</sup>

<sup>1</sup>Department of Architectural Engineering, College of Engineering, Sejong University, 143-747, Seoul, Korea

<sup>2</sup>Research Institute of Industrial Technology, Pusan National University, 609-735, Busan, Korea

(Received July 5, 2013, Revised May 29, 2015, Accepted September 7, 2015)

**Abstract.** This study presents optimizing structural topology patterns using regularization of Heaviside function. The present method needs not filtering process to typical SIMP method. Using the penalty formulation of the SIMP approach, a topology optimization problem is formulated in co-operation, i.e., couple-signals, with design variable values of discrete elements and a regularized Heaviside step function. The regularization of discontinuous material distributions is a key scheme in order to improve the numerical problems of material topology optimization with 0 (void)-1 (solid) solutions. The weak forms of an equilibrium equation are expressed using a coupled regularized Heaviside function to evaluate sensitivity analysis. Numerical results show that the incorporation of the regularized Heaviside function and the SIMP leads to convergent solutions. This method is tested using several examples of a linear elastostatic structure. It demonstrates that improved optimal solutions can be obtained without the additional use of sensitivity filtering to improve the discontinuous 0-1 solutions, which have generally been used in material topology optimization problems.

**Keywords:** optimization; topology patterns; SIMP; filtering process, regularized Heaviside function

---

### 1. Introduction

Nowadays, topology optimization is being extensively studied and used in the engineering field to solve problems in areas such as aeronautics, automobiles, microstructure systems and mechanism design. Topology optimization generates the optimal shape of a mechanical structure (Rozvany 2001, Lee *et al.* 2015a, 2015b, 2015c, Bendsoe and Kikuchi 1988). The structural shape is generated within a pre-defined design space. In addition, the user provides structural supports and loads. Without further decisions and guidance from the user, the method will form the structural shape, thus providing a first idea of an efficient geometry. Therefore, topology optimization is a much more flexible design tool than conventional structural shape optimization (Zienkiewicz 1973), where only a selected part of the boundary is varied without any chance to generate a lightness hole. The goal of topology optimization is to seek an optimal material distribution (for example, the density distribution), within a design domain that minimizes a given

---

\*Corresponding author, Senior Researcher, E-mail: [shinsumi82@pusan.ac.kr](mailto:shinsumi82@pusan.ac.kr)

<sup>a</sup>Professor

objective function and satisfies constraint conditions. Here the design domain is defined by a continuum discretized by finite elements. The optimization algorithm assigns a design variable to each finite element. These design variables of discrete elements range continuously from 0 to 1 thus from voids and solids.

Kohn and Strang (1986) stated that the main difficulty in topology optimization is its ill-posed problems. Therefore, the 0-1 formulation with a discrete finite element form is mesh-dependent and its solution may be singular. In this context, Sigmund and Petersson (1998) proved that solutions to topology optimization problems often create numerical instability, i.e., singularities of the solutions associated with mesh-dependence, checkerboards, and local minima (Diaz and Sigmund 1995).

To overcome these problems and obtain the desired material distributions, a well-known approach is available for solving well-posed problems. It is based on homogenization theory (Fujii *et al.* 2001) as devised by Bendsøe and Kikuchi (1988) in which a material model with micro-scale voids is introduced and the topology optimization problem is defined by searching for the optimal porosity as introduced by Bendsøe and Haber (1993), Bendsøe (1989), Eschenauer *et al.* (1994), Rozvany *et al.* (1992). Many approaches to this homogenization method have been investigated; for example, the so-called “Solid Isotropic Microstructure with Penalization” (SIMP) approach by Sigmund (2001), Patnaik *et al.* (2005), Diaz and Bendsøe (1992), Bendsøe and Sigmund (1999), Lee *et al.* (2014a), Bourdin (2001). The SIMP approach has both a simple structural analysis and optimization, selectively suppresses the porous regions by adjusting the penalty, and handles a variety of design conditions, i.e., combinations of deflections, stresses, natural frequencies and stability constraints for several load conditions. However, the remaining major physical difficulty is the weak relationship between design variables and Young’s modulus for realistic requirements. The level set method (Wang *et al.* 2003, Wang *et al.* 2004, Osher and Fedkiw 2001, Zhu *et al.* 2015) which reduces, as mentioned, “the weak relationship between design variables and Young’s” by eliminating gray regions (density between 0 and 1) without filtering technique.

The approach introduced in this paper addresses nonlinear the decreasing stiffness difference for each finite element. We propose that in addition to the penalty formulation in the SIMP approach, a regularized Heaviside function be used that is dependent on a design variable of design domain. This element-based coupled value is then assigned as a constant value onto each finite element. This simple change, coupled with an appropriate regularized Heaviside function, appears to yield mesh independent and checkerboard-free solutions. These benefits are realized without using any additional filter methods in the SIMP approach.

Using a design variable dependent, regularized Heaviside function in the topology optimization is not a new idea. Belytschko *et al.* (2003), Guest *et al.* (2004), Kawamoto *et al.* (2011) reported success using the regularized Heaviside function, which was introduced by Wang *et al.* (2003, 2004), Osher and Fedkiw (2001), and implicit functions to describe the topology. The approach presented here differs from theirs in that the regularized Heaviside function is also used as another multiplied penalty function in the SIMP approach, for instance, as couple-signals. During the topology optimization procedures, the 0-1 solutions in the design domain are signal sets of a typical Heaviside function, as shown in Fig. 1. The regularized Heaviside function has been expressed using diverse versions by Belytschko *et al.* (2003), Berthelsen (2002), and Moog (2000) and has smoothed values ranging from 0.5 to 1.0 based on the density values of the material phases of design domain. This is shown in Figs. 2 and 3. This function is used to solve the equilibrium equation and applied to the sensitivity analysis (or derivatives of the objective

functions and constraints) of the topology optimization algorithm.

The layout of this study is as follows. In Section 2, the goal and intuitive idea of this study is discussed, including its theoretical and numerical aspects. Through this conceptual representation of a couple-signal of the design domain, formulations of the well-known two-phase material topology optimization problem are evolved in Section 3. In Section 4, a sensitivity analysis of the objective function of the proposed method is introduced using the adjoint method of Lagrangian multiplier. Section 4 also includes a discretization of the continuous design domain. In Section 5, numerical interactions of the couple-signal approach are presented in the design domain. The couple-signal method using the SIMP approach is applied to numerical sample problems in Section 6 and conclusions are given in Section 7.

## 2. Goal and intuitive idea

In continuous formulations of the material topology optimization problem, the design is given by a continuous scalar function,  $\Phi$ , from the fixed design domain,  $\Omega_x \subseteq \mathbb{R}^n$  ( $n=2$  or  $3$ ), to the allowed material density,  $0 \leq \Phi \leq 1$ . After the discretization processes such as the finite element analysis of the continuous domain, the material density,  $\Phi_i$ , is assigned to each finite element and is defined by applying a penalty contour to the design variable field, as in the so-called “power law approach” or SIMP approach.

According to this approach, the material density distribution affects the element stiffness. Thus, the stiffness-density relation may be expressed in terms of Young’s modulus,  $E$ , i.e.,  $E_i$  is given by the updated density,  $\Phi_i$ , of each finite element and is defined as

$$E_i(\Phi_i) = E_0 \left( \frac{\Phi_i}{\Phi_0} \right)^\beta \quad \beta \geq 1, \quad i = 1, \dots, n, \quad n = \text{total number of elements} \quad (1)$$

where  $E_0$  and  $\Phi_0$  are the nominal values of Young’s modulus and material density, respectively. The penalty parameter,  $\beta$ , penalizes the intermediate material. For example, an isotropic material model with a plane stress (such as a wall structure) has been used without losing generality, so that

$$C_i = \frac{E_i(\Phi_i)}{1-\nu^2} \begin{bmatrix} 1 & \nu & 0 \\ \nu & 1 & 0 \\ 0 & 0 & \frac{1-\nu}{2} \end{bmatrix} \quad (2)$$

where  $C_i$  is a material tensor of each finite element,  $i$ , and includes the updated term of Young’s modulus,  $E_i$ , given by the updated element density,  $\Phi_i$ .  $\nu$  is Poisson’s ratio. Here, the minimal strain energy on a linear elastostatic structure has been used as an objective function of topology optimization and is generally defined as

$$\text{Minimize } f = \frac{1}{2} \int_{\Omega_x} \boldsymbol{\varepsilon}^T C_i \boldsymbol{\varepsilon} \, d\Omega_x \quad (3)$$

Within each element of the structure, material property distributions such as densities remain

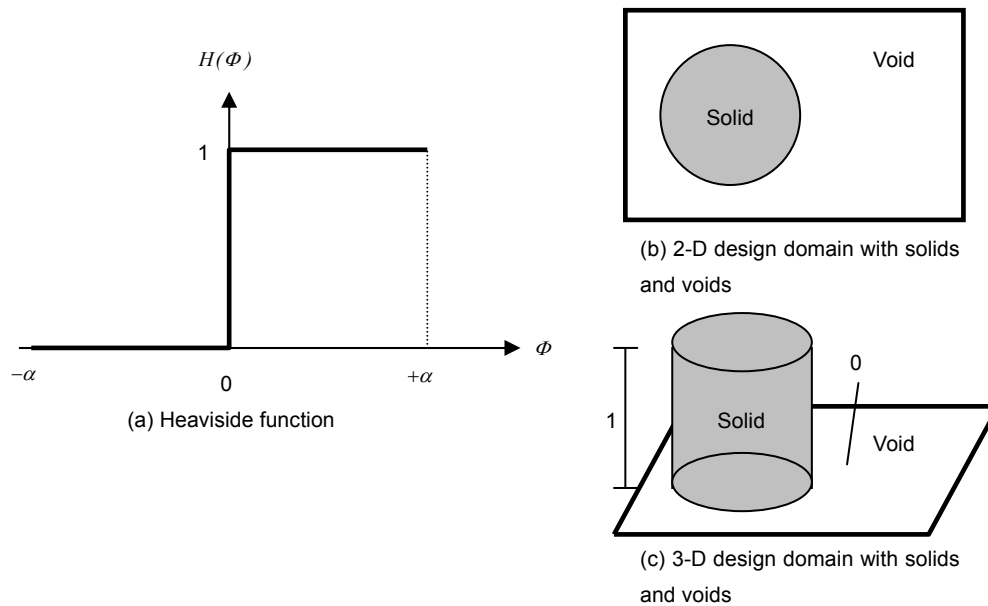


Fig. 1 Heaviside function with 0-1 formulation and its expression in design domain

constant values of  $0 \leq \Phi_i \leq 1$ . The material tensor,  $C_i$ , includes an indication function as a “self-existing signal” of 0 or 1 in the SIMP approach. That is, if material density exists in a design domain with discretized finite elements, part of the design domain is characterized by 1, otherwise, 0. Therefore, additional signals are not normally used in the same design domain. Therefore, Eq. (3) can be rewritten as including generalized Heaviside function

$$\text{Minimize } f = \frac{1}{2} \int_{\Omega_x} H(\Phi_i) \boldsymbol{\varepsilon}^T C_i \boldsymbol{\varepsilon} d\Omega_x \quad (4)$$

where due to the fixed ranges of element material density,  $-1 \leq \rho (= 2\Phi_i - 1) \leq 1$ , the generalized Heaviside function is defined as follows

$$H(\rho) = \begin{cases} 0 & \text{if } \rho < 0 \\ \frac{1}{2} & \text{if } \rho = 0 \\ 1 & \text{if } \rho > 0 \end{cases} \quad (5)$$

The Heaviside function with a 0-1 formulation and its expression in the design domain are shown in Fig. 1. However, when solving the topology optimization formulations numerically, large jumps in density,  $\Phi_i$ , across the interface (for example, at the boundary) may cause numerical instabilities, such as singularities. Moreover, the first derivative of the objective, Eq. (4), would make it unworkable since the derivative of the Heaviside function is the Dirac delta function. Special care must, therefore, be taken.

In order to prevent these numerical difficulties, Berthelsen (2002) popularized the practice of introducing an interface thickness to smooth the density at the interface. This can be done by

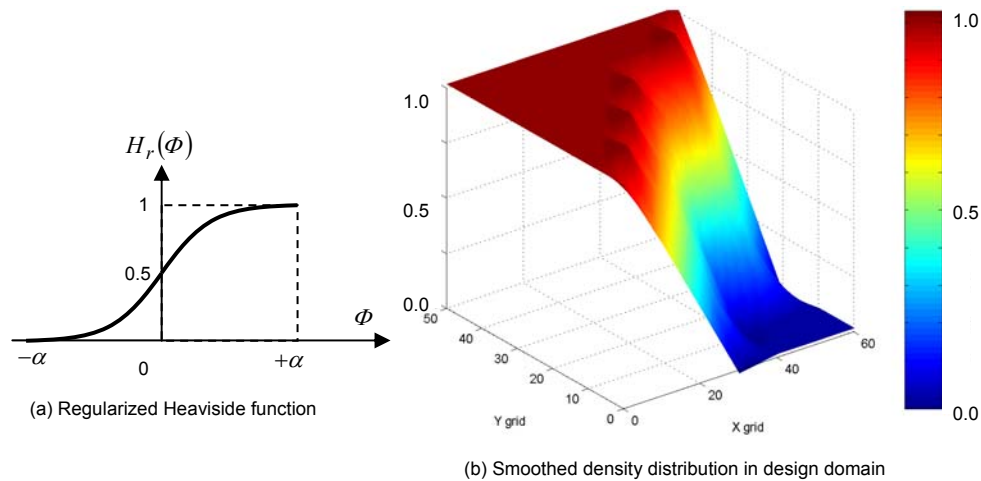


Fig. 2 Regularized Heaviside function with 0-1 formulation and smoothed density distributions in a design domain

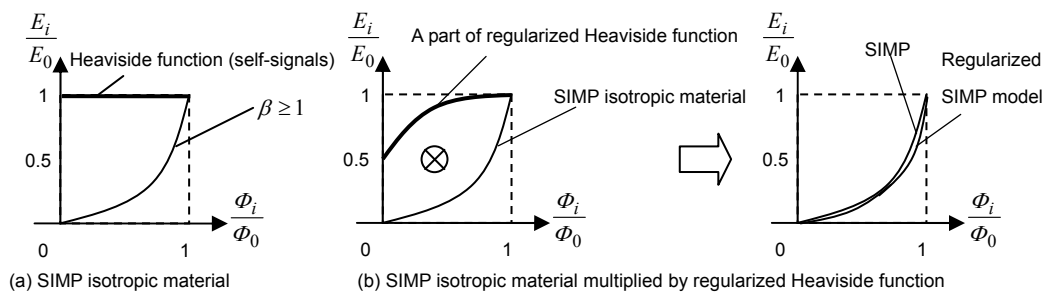


Fig. 3 SIMP isotropic material model multiplied by regularized Heaviside function-couple signals

replacing the Heaviside function introduced above by a smoothed, regularized Heaviside function,  $H_r(\Phi_i)$ , defined as follows

$$H_r(\Phi_i) = \begin{cases} \frac{1}{2} & \text{if } \Phi_i = 0 \\ \frac{3}{4} \left[ \frac{\Phi_i}{\alpha} - \frac{1}{3} \left( \frac{\Phi_i}{\alpha} \right)^3 \right] + \frac{1}{2} & \text{if } 0 < \Phi_i \leq \alpha \end{cases} \quad (6)$$

Here, the regularized Heaviside function of Eq. (6) was introduced by Wang *et al.* (2004); furthermore, in numerical calculations, it is assumed that the interface thickness should be set at  $\alpha=1.0$  since the maximal value of material densities in the design domain is 1.0. The conceptual expression of the regularization of a Heaviside function is shown in Fig. 2.

Consequently, this regularized Heaviside function is smoothed over the interface thickness. To perform the sensitivity analysis of the topology optimization problem, a derivative of the regularized Heaviside function must be introduced here. The regularized Dirac delta function,  $\delta_r(\Phi_i)$ , at a fixed range of  $0 \leq \Phi_i \leq 1$  is defined as follows

$$\delta_r(\Phi_i) = \frac{\partial H_r(\Phi_i)}{\partial \Phi_i} \quad (7)$$

or

$$\delta_r(\Phi_i) = \begin{cases} \frac{3}{4\alpha} & \text{if } \Phi_i = 0 \\ \frac{3}{4\alpha} \left[ 1 - \left( \frac{\Phi_i}{\alpha} \right)^2 \right] & \text{if } 0 < \Phi_i \leq \alpha \end{cases} \quad (8)$$

Finally, by using the regularized Heaviside function of Eq. (6), the objective function of Eq. (4) can be rewritten as follows

$$\text{Minimize } f_r = \frac{1}{2} \int_{\Omega_x} H_r(\Phi_i) \boldsymbol{\varepsilon}^T \mathbf{C}_i \boldsymbol{\varepsilon} \, d\Omega_x \quad (9)$$

where the renewal objective function,  $f_r$ , is defined by the regularization of a Heaviside function. The scalar strain energy of Eq. (9) takes heavier values than the objective function value of Eq. (3) of the typical SIMP approach. This requirement is because the relative stiffness of finite elements decreases as the relative displacement increases. Compared to the conventional SIMP approach of self-existing signals, the regularized Heaviside function with couple-signals and the relationship of the density-stiffness of the SIMP approach are shown in Fig. 3.

The key result of the regularized SIMP approach with couple-signals is that the relative difference of each element stiffness decreases during the optimization processes. Therefore, the regularized SIMP approach eliminates the singularities that would otherwise arise in the finite element analysis when regions of low density material,  $\Phi_i \rightarrow 0$ , appear in the optimization processes. The higher value of the elastic strain energy is converged and poses no computational problems in the presence of low density elements for most topology optimization problems, i.e., structures with small deformations.

### 3. Two-Phase material topology optimization problem: displacement approach as a minimization of total potential energy

In this study, a linear elastostatic structure was used in order to describe the problem of the structural two-phase material topology optimization. Let  $\Omega_x \subseteq \mathfrak{R}^n$  ( $n=2$  or  $3$ ) be a design domain occupied by isotropic material. The boundary condition of  $\Omega_x$  is composed of three parts, i.e.,  $\Gamma = \partial\Omega_x = \Gamma_x \cup \Gamma_t \cup \Gamma_u$ : the Neumann boundary condition on  $\Gamma_t$ ; the Dirichlet condition on  $\Gamma_u$ ; and the traction free boundary segment on  $\Gamma_x$ . The first and second parts are written as follows

$$\bar{\mathbf{t}} = \mathbf{t}_0 \quad \text{on } \Gamma_t \quad (10)$$

$$\bar{\mathbf{u}} = \mathbf{u}_0 \quad \text{on } \Gamma_u \quad (11)$$

where  $\mathbf{t}_0$  and  $\mathbf{u}_0$  are given traction forces (or surface loads) and displacement fields, respectively. The field condition of  $\Omega_x$  consists of balanced, constitutive and kinematic conditions, and they are

expressed as respectively

$$\operatorname{div} \boldsymbol{\sigma} + \bar{\mathbf{b}} = 0 \quad (12)$$

$$\boldsymbol{\sigma} = \mathbf{C}\boldsymbol{\varepsilon} \quad (13)$$

$$\boldsymbol{\varepsilon} = \mathbf{L}\mathbf{u} \quad (14)$$

where  $\bar{\mathbf{b}}$  is a body force and it is assumed that the stress  $\boldsymbol{\sigma}$  depends only on actual deformation. In linear elastic isotropic structures, the material tensor,  $\mathbf{C}$ , is symmetric after a discretized process; therefore, the continuous displacement field,  $\mathbf{u}$ , in  $\Omega_x$  is a unique solution.

The schematic of the two-phase material topology optimization of a solid structure with specified field and boundary conditions is shown in Fig. 4.

The principle of virtual displacements uses an ensured satisfaction of equilibrium conditions within the weak form. The virtual work principle can be written as follows if the virtual quantities  $\delta\mathbf{u}$  and  $\delta\boldsymbol{\varepsilon}$  are considered as variations (or differentials) of the real quantities.

$$\delta\omega(\delta\mathbf{u}, \mathbf{u}, \Phi) = \delta\omega^i(\delta\mathbf{u}, \mathbf{u}, \Phi) + \delta\omega^a(\delta\mathbf{u}, \mathbf{u}) = 0 \quad \delta\mathbf{u}, \mathbf{u}, \Phi \in V_u(\Omega_x) \subseteq H^1(\Omega_x) \quad (15)$$

where  $\delta\omega^i$  and  $\delta\omega^a$  denote virtual internal and virtual external work, respectively.  $\Phi$  is a property of material densities. The virtual internal work,  $\delta\omega^i$ , is expressed by virtual strains,  $\delta\boldsymbol{\varepsilon}$ , stresses,  $\boldsymbol{\sigma}$ , and a free-selected regularized Heaviside function,  $H_r$ , depending on the material density as follows

$$\delta\omega^i = \int_{\Omega_x} \delta\boldsymbol{\varepsilon}^T \boldsymbol{\sigma} H_r(\Phi) \, d\Omega_x \quad (16)$$

where it is assumed that the material density is independent of external forces, i.e., body and traction forces. The traction forces are conservative (or independent of displacement fields).

Therefore, without the expression of a free-selected Heaviside function, the virtual external work,  $\delta\omega^a$ , is given by body forces,  $\bar{\mathbf{b}}$ , traction forces,  $\bar{\mathbf{t}}$ , and virtual displacement fields,  $\delta\mathbf{u}$ , as follows

$$\delta\omega^a = - \int_{\Omega_x} \delta\mathbf{u}^T \bar{\mathbf{b}} \, d\Omega_x - \int_{\Gamma_t} \delta\mathbf{u}^T \bar{\mathbf{t}} \, d\Gamma_t \quad (17)$$

Using Eq. (16) and (17), the equilibrium conditions of Eq. (15) can be rewritten as

$$\int_{\Omega_x} \delta\boldsymbol{\varepsilon}^T \boldsymbol{\sigma} H_r(\Phi) \, d\Omega_x = \int_{\Omega_x} \delta\mathbf{u}^T \bar{\mathbf{b}} \, d\Omega_x + \int_{\Gamma_t} \delta\mathbf{u}^T \bar{\mathbf{t}} \, d\Gamma_t \quad (18)$$

Eq. (15) indicates that for equilibrium to be ensured the total potential energy must be stationary for variations of admissible displacements. It can be shown that in stable elastic situations the total potential energy is not only stationary but is a minimum.

The weak form of the equilibrium can be differentiated by the principle of minimum potential energy as follows

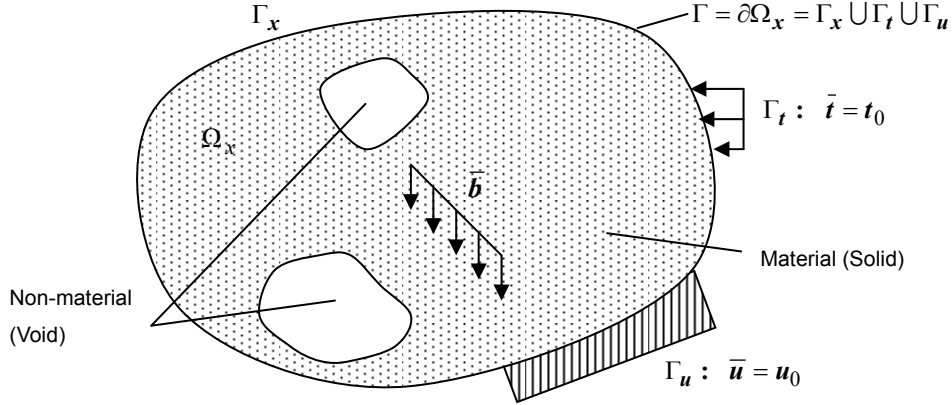


Fig. 4 Schematic of two-phase material topology optimization of a solid structure with specified field and boundary conditions

$$\text{Minimize } \Pi(\mathbf{u}, \Phi) \rightarrow \delta \Pi(\mathbf{u}, \Phi) = 0 \quad \delta \mathbf{u}, \mathbf{u}, \Phi \in V_u(\Omega_x) \subseteq H^1(\Omega_x) \quad (19)$$

Please note that by the principle of minimum potential energy, the objective function can be written as

$$\begin{aligned} \Pi(\mathbf{u}, \Phi) &= \Pi^i(\mathbf{u}, \Phi) + \Pi^a(\mathbf{u}, \Phi) \\ &= \frac{1}{2} \int_{\Omega_x} \delta \boldsymbol{\varepsilon}^T \mathbf{C} \boldsymbol{\varepsilon} H_r(\Phi) \, d\Omega_x - \int_{\Omega_x} \delta \mathbf{u}^T \bar{\mathbf{b}} \, d\Omega_x - \int_{\Gamma_t} \delta \mathbf{u}^T \bar{\mathbf{t}} \, d\Gamma_t \\ &= -\frac{1}{2} \int_{\Omega_x} \delta \boldsymbol{\varepsilon}^T \mathbf{C} \boldsymbol{\varepsilon} H_r(\Phi) \, d\Omega_x \end{aligned} \quad (20)$$

where the continuous material tensor,  $\mathbf{C}$ , depends on the relationship of material density-stiffness of the typical SIMP approach according to the numerical application that a continuous design domain is discretized into finite numbers of elements. The discontinuous Heaviside function is regularized as a smoothed form. For this purpose, the discretization of the continuous form of the objective function of Eq. (20) can be defined as Eq. (9).

The inequality optimization condition is  $0 \leq \Phi \leq 1$ , and an equality constraint describes the limit on the required amount of materials in terms of the constant mass  $M_{ref}$  of the design domain as follows

$$\int_{\Omega_x} \Phi \, d\Omega_x - M_{ref} = 0 \quad (21)$$

The general problem of structural topology optimization is specified by the objective function and constraints. The objective function is expressed as Eq. (20) and the constraint conditions are

the linear elastic equilibrium of Eq. (18) written in a weak form satisfying the field and boundary conditions and mass constraints of Eq. (21).

#### 4. Analytical sensitivity analysis using variational method

In general, the sensitivity of optimization problems such as objective functions or constraints can be calculated by analytical or numerical analyses. In terms of numerical errors of the sensitivity calculations, when compared with the exact solutions, analytical method is better. This method is classified as variational and discrete methods. The variational method is more efficient numerically than the discrete method in case definitions of optimization problems and design variables are fixed. Therefore, the variational method has been used here.

Since continuous displacement fields depend on the design variables,  $s$ , (for instance, material densities), the total derivative of the objective function consists of parts of an explicit partial derivative and implicit partial derivative, and the formulation is defined by Haftka and Guerdal (1992), Haug *et al.* (1986) as follows

$$\nabla_s f = \nabla_s^{ex} f + \bar{\nabla}_u f^T \nabla_s \mathbf{u} \tag{22}$$

According to the general sensitivity formulation of Eq. (22), the total partial derivative of the objective function associated with a regularized Heaviside function with respect to design variables is written as follows

$$\begin{aligned} \nabla_s f_r = & \underbrace{\frac{1}{2} \int_{\Omega_x} \boldsymbol{\varepsilon}^T \nabla_s \mathbf{C}(\Phi) \boldsymbol{\varepsilon} H_r(\Phi) d\Omega_x + \frac{1}{2} \int_{\Omega_x} \boldsymbol{\varepsilon}^T \mathbf{C}(\Phi) \boldsymbol{\varepsilon} \delta_r(\Phi) d\Omega_x}_{\text{explicit derivative}} \\ & + \underbrace{\frac{1}{2} \int_{\Omega_x} \boldsymbol{\varepsilon}^T \mathbf{C}(\Phi) \nabla_u \boldsymbol{\varepsilon} H_r(\Phi) \nabla_s \mathbf{u} d\Omega_x}_{\text{implicit derivative}} \end{aligned} \tag{23}$$

By using a derivative of an equilibrium equation of Eq. (18) satisfying field and boundary conditions, the term of a derivative of continuous displacement fields,  $\nabla_s \mathbf{u}$ , with respect to design variables can be written as

$$\begin{aligned} \int_{\Omega_x} \delta \mathbf{u}^T \mathbf{L}^T \mathbf{C}(\Phi) \mathbf{L} H_r(\Phi) \nabla_s \mathbf{u} d\Omega_x = & \int_{\Omega_x} \delta \mathbf{u}^T \nabla_s \bar{\mathbf{b}} d\Omega_x + \int_{\Gamma_t} \delta \mathbf{u}^T \nabla_s \bar{\mathbf{t}} d\Gamma_t \\ & - \int_{\Omega_x} \delta \mathbf{u}^T \nabla_s \mathbf{L}^T \mathbf{C}(\Phi) \mathbf{L} \mathbf{u} H_r(\Phi) d\Omega_x - \int_{\Omega_x} \delta \mathbf{u}^T \mathbf{L}^T \nabla_s \mathbf{C}(\Phi) \mathbf{L} \mathbf{u} H_r(\Phi) d\Omega_x \\ & - \int_{\Omega_x} \delta \mathbf{u}^T \mathbf{L}^T \mathbf{C}(\Phi) \nabla_s \mathbf{L} \mathbf{u} H_r(\Phi) d\Omega_x - \int_{\Omega_x} \delta \mathbf{u}^T \mathbf{L}^T \mathbf{C}(\Phi) \mathbf{L} \mathbf{u} \delta_r(\Phi) d\Omega_x \end{aligned} \tag{24}$$

In order to calculate a derivative of continuous displacement fields,  $\nabla_s \mathbf{u}$ , an adjoint method is used here. The adjoint method does not directly calculate derivatives of continuous displacement fields serving a large number of computational costs. According to the adjoint method, a new objective function is defined as follows

$$\tilde{f}_r = f_r - \lambda \left[ \int_{\Omega_x} \delta \boldsymbol{\varepsilon}^T \boldsymbol{\sigma} H(\Phi) \, d\Omega_x - \int_{\Omega_x} \delta \mathbf{u}^T \bar{\mathbf{b}} \, d\Omega_x - \int_{\Gamma_t} \delta \mathbf{u}^T \bar{\mathbf{t}} \, d\Gamma_t \right] \quad (25)$$

where the renewed objective function,  $\tilde{f}_r$ , has an additional 0-term (for example, static equilibrium), which is multiplied by a Lagrangian multiplier,  $\lambda$ .

The derivative of the Lagrangian multiplier disappears because of the 0-term. Therefore the derivative of Eq. (25) is written as

$$\begin{aligned} \nabla_s \tilde{f}_r &= \nabla_s^{ex} \tilde{f}_r + \bar{\nabla}_u \tilde{f}_r^T \nabla_s \mathbf{u} - \lambda \underbrace{\int_{\Omega_x} \delta \mathbf{u}^T L^T \mathbf{C}(\Phi) \mathbf{L} H_r(\Phi) \, \nabla_s \mathbf{u} \, d\Omega_x}_{(a)=0} \\ &- \lambda \int_{\Omega_x} \delta \mathbf{u}^T \nabla_s L^T \mathbf{C}(\Phi) \mathbf{L} u H_r(\Phi) \, d\Omega_x - \lambda \int_{\Omega_x} \delta \mathbf{u}^T L^T \nabla_s \mathbf{C}(\Phi) \mathbf{L} u H_r(\Phi) \, d\Omega_x \\ &- \lambda \int_{\Omega_x} \delta \mathbf{u}^T L^T \mathbf{C}(\Phi) \nabla_s \mathbf{L} u H_r(\Phi) \, d\Omega_x - \lambda \int_{\Omega_x} \delta \mathbf{u}^T L^T \mathbf{C}(\Phi) \mathbf{L} u \delta_r(\Phi) \, d\Omega_x \\ &+ \lambda \int_{\Omega_x} \delta \mathbf{u}^T \nabla_s \bar{\mathbf{b}} \, d\Omega_x + \lambda \int_{\Gamma_t} \delta \mathbf{u}^T \nabla_s \bar{\mathbf{t}} \, d\Gamma_t \end{aligned} \quad (26)$$

Lagrangian multipliers,  $\lambda$ , have arbitrary values. We can select a specific Lagrangian multiplier value in Eq. (26) in order to remove a derivative of the continuous displacement fields, which is numerically very expensive. Therefore, a specific equation  $(a)=0$  in Eq. (26) is produced, including the specific Lagrangian multiplier value.

After discretization of a continuous design domain, the specific equation with a satisfactory Lagrangian multiplier is expressed as

$$\hat{\mathbf{u}}^T \int_{\Omega_\xi} \mathbf{B}^T \mathbf{C} \mathbf{B} |J| H_r(\Phi) \, d\Omega_\xi \nabla_s \hat{\mathbf{u}} - \lambda \delta \hat{\mathbf{u}}^T \int_{\Omega_\xi} \mathbf{B}^T \mathbf{C} \mathbf{B} |J| H_r(\Phi) \, d\Omega_\xi \nabla_s \hat{\mathbf{u}} = 0 \quad (27)$$

Through Eq. (27), a required Lagrangian multiplier value is written as follows

$$\lambda = \hat{\mathbf{u}}^T \left( \delta \hat{\mathbf{u}}^T \right)^{-1} \quad (28)$$

Through the use of Eq. (27) and (28), in a discretized design domain, a total partial derivative of the objective function by the design variable is finally written as follows

$$\begin{aligned} \nabla_s \tilde{f}_r = & \frac{1}{2} \hat{\mathbf{u}}^T \int_{\Omega_\xi} \mathbf{B}^T \nabla_s \mathbf{C}(\Phi) \mathbf{B} |\mathbf{J}| H_r(\Phi) d\Omega_\xi \hat{\mathbf{u}} + \frac{1}{2} \hat{\mathbf{u}}^T \int_{\Omega_\xi} \mathbf{B}^T \mathbf{C}(\Phi) \mathbf{B} |\mathbf{J}| \delta(\Phi) d\Omega_\xi \hat{\mathbf{u}} \\ & - \hat{\mathbf{u}}^T \left[ \int_{\Omega_\xi} \nabla_s \mathbf{B}^T \mathbf{C}(\Phi) \mathbf{B} |\mathbf{J}| H_r(\Phi) d\Omega_\xi \hat{\mathbf{u}} + \int_{\Omega_\xi} \mathbf{B}^T \nabla_s \mathbf{C}(\Phi) \mathbf{B} |\mathbf{J}| H_r(\Phi) d\Omega_\xi \hat{\mathbf{u}} + \int_{\Omega_\xi} \mathbf{B}^T \mathbf{C}(\Phi) \nabla_s \mathbf{B} |\mathbf{J}| H_r(\Phi) d\Omega_\xi \hat{\mathbf{u}} \right. \\ & \left. + \int_{\Omega_\xi} \mathbf{B}^T \mathbf{C}(\Phi) \mathbf{B} |\mathbf{J}| \delta_r(\Phi) d\Omega_\xi \hat{\mathbf{u}} - \int_{\Omega_\xi} \mathbf{N}^T \nabla_s \bar{\mathbf{b}} |\mathbf{J}| d\Omega_\xi - \int_{\Omega_\eta} \mathbf{N}^T \nabla_s \bar{\mathbf{t}} \sqrt{|G_e|} d\Omega_\eta \right] \end{aligned} \quad (29)$$

Under the assumptions that external forces  $\bar{\mathbf{b}}$ ,  $\bar{\mathbf{t}}$ , differential matrix,  $\mathbf{L}$ , and a Jacobi matrix,  $\mathbf{J}$ , are independent of the design variables, the total partial derivative of the objective function can be simply written as follows

$$\nabla_s \tilde{f}_r = -\frac{1}{2} \hat{\mathbf{u}}^T \int_{\Omega_\xi} \mathbf{B}^T \nabla_s \mathbf{C}(\Phi) \mathbf{B} |\mathbf{J}| H_r(\Phi) d\Omega_\xi \hat{\mathbf{u}} - \frac{1}{2} \hat{\mathbf{u}}^T \int_{\Omega_\xi} \mathbf{B}^T \mathbf{C} \mathbf{B} |\mathbf{J}| \delta_r(\Phi) d\Omega_\xi \hat{\mathbf{u}} \quad (30)$$

### 5. Finite element stiffness and structural behaviors in regularization

The couple-signal method using the regularized Heaviside function involves significant reductions in element stiffness. The integral of the discretized design domain with a material phase takes the value 0.8125, not 1, when Eq. (6) is regularization and used in the design domain. The area (in 2D) loss (for example, the smoothed boundary value at each element domain), results in the loss of stiffness or updated Young’s modulus. At the same time, this numerical phenomenon includes especially important decreases in relative stiffness differences between each neighboring

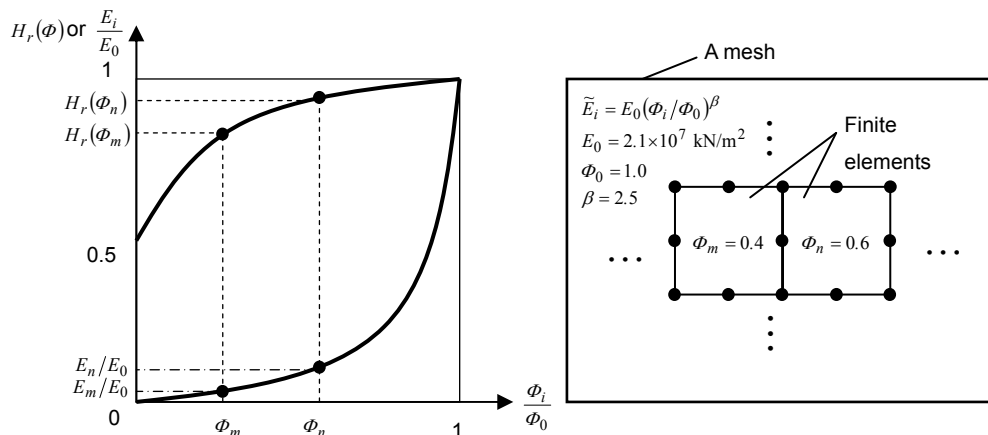


Fig. 5 Relative stiffness of each neighboring element in original SIMP and regularized SIMP

Table 1 Relative stiffness of each neighboring element in original SIMP and regularized SIMP

	$E_m$	$E_n$	error
Original SIMP	2125050.588	5855950.820	3730900.232
Regularized SIMP	1666039.661	5246931.935	3580892.274

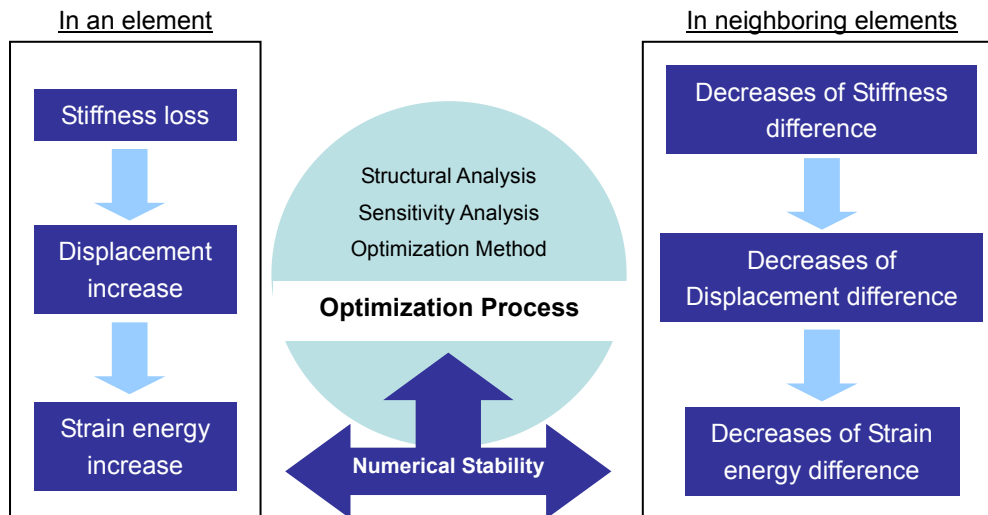


Fig. 6 Optimization procedures affected by some stiffness loss in regularized SIMP

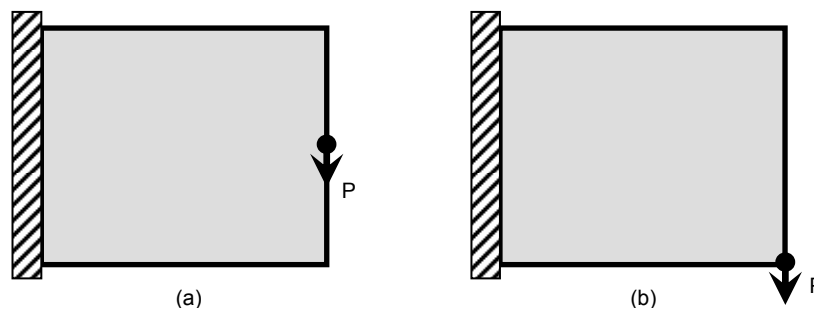


Fig. 7 Problem types-2D wall structures

element. Therefore, during the optimization procedures, an updated structure's behavior validates numerical stabilities. The results of a numerically experimental test to prove these characteristics are shown in Figs. 5 and 6 and Table 1.

## 6. Numerical applications and discussion

As test examples, the elastostatic 2D wall structures as shown in Fig. 7 are considered to validate the proposed method. All examples were solved using eight-node square structured meshes with quadratic shape functions of a serendipity family. For numerical integration of the

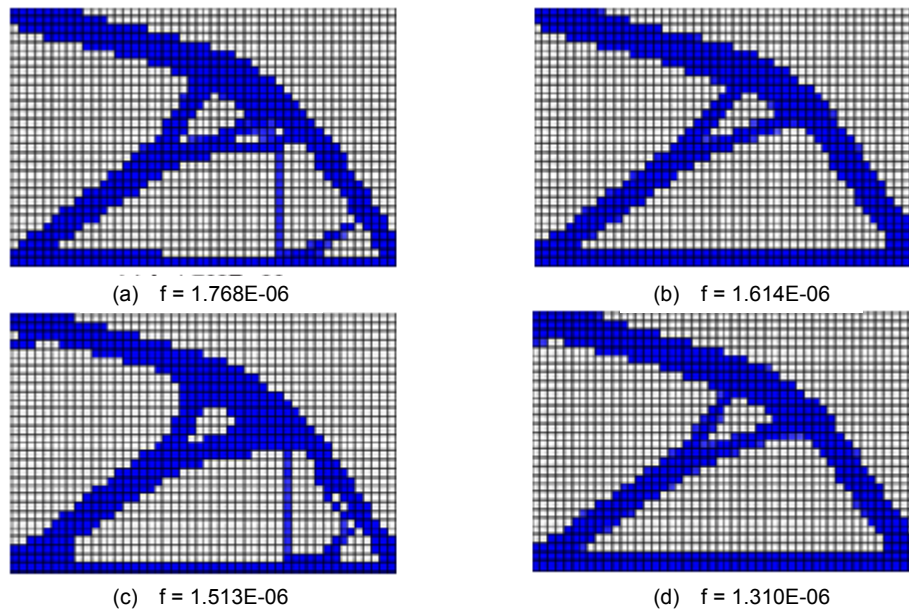


Fig. 8 Optimal density distributions of Fig. 7(a)- (a) Original SIMP (b) Filtered SIMP (c) Regularized SIMP (d) Filtered and Regularized SIMP

discretized elements of the design domain, a  $2 \times 2$  Gauss quadrature was used.

The material properties are Young's module  $E=2.1 \times 10^7$  kN/m<sup>2</sup> and Poisson's ratio  $\nu=0.3$ . Plane stress is assumed in 2D and the loading is in a concentrated load of  $P=1.0$  kN. The exponent,  $k=2.5$ , and updated material density,  $0 \leq \Phi_i \leq 1$ , are used in the SIMP method in all cases. The initial values of the density variables are set to be  $\Phi_0=0.3$  for all elements. The filter exponent  $\beta=2.2$  and a radius  $r=\max(\Delta x, \Delta y)+\gamma$  (in example 6.1 (a):  $\gamma=10^{-3}$ , otherwise,  $\gamma=10^{-2}$ .  $\gamma$  is a fine parameter and is chosen for the Filter method (Sigmund 1994). The  $\Delta x$  and  $\Delta y$  are mesh sizes of x-direction and y-direction, respectively. 30% constraint mass is used for the constraint condition.

### 6.1 Two-Phase material topology optimization of 2D wall structures

The problem of material topology optimization shown in Fig. 7 includes diving boards, an airplane wing, posts, poles, masts, trees, and branches. A  $48 \times 30$  mesh is used in problem (a), and a  $30 \times 60$  mesh in problem (b). The final results of the topology optimization problem of Fig. 7 are shown in Figs. 8 and 9, respectively. In Figs. 8 and 9, (a) is a solution for the original SIMP, (b) a solution for a SIMP using filtering, (c) a solution for a SIMP using couple-signals, the so-called "regularized" SIMP, and (d) a solution for a SIMP using filtering and couple-signals.

As can be seen, the use of a regularized Heaviside function for couple-signals as shown in (c) and (d) of Figs. 8 and 9 results in improved optimal solutions with the best minimums of converged objective function values and numerical stabilities.

### 6.2 Various types of regularized heaviside function for regularized SIMP

To calculate example 6.1, transcendental and first polynomial regularized Heaviside functions

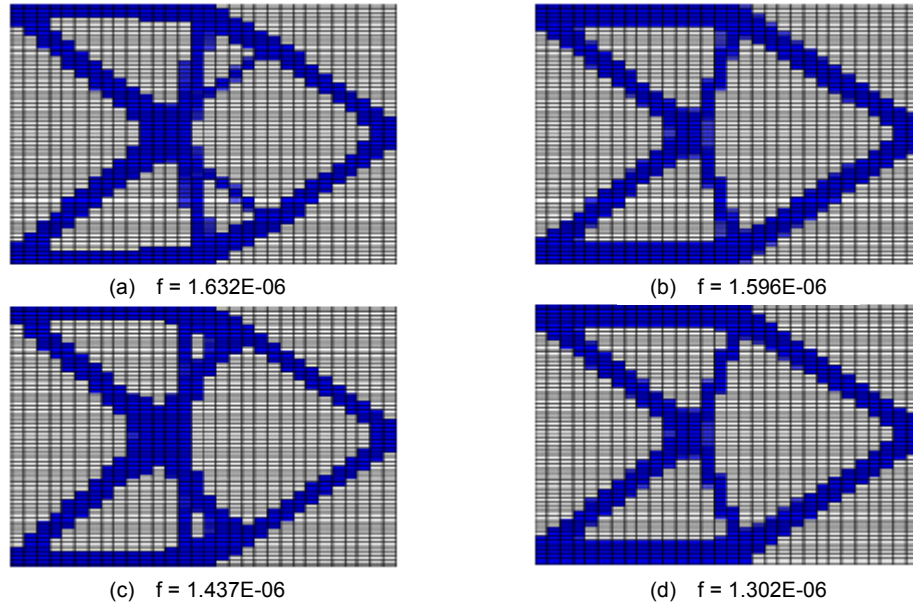


Fig. 9 Optimal density distributions of Fig. 7 (b) - (a) Original SIMP (b) Filtered SIMP (c) Regularized SIMP (d) Filtered and Regularized SIMP

were solved for the proposed regularized SIMP approach. Cases 2~5 were introduced in recent literature, including Case 1 of Eqs. (6) and (8). The regularized Heaviside function and its Dirac delta function of Case 2 introduced by Osher and Paragios (2003) are defined as follows, respectively.

$$H_r(\Phi_i) = \begin{cases} \frac{1}{2} & \text{if } \Phi_i = 0 \\ \frac{1}{2} + \frac{2}{\pi} \arctan\left(\frac{\Phi_i}{\alpha}\right) & \text{if } 0 < \Phi_i \leq \alpha \end{cases} \quad (31)$$

$$\delta_r(\Phi_i) = \begin{cases} \frac{2}{\pi\alpha} & \text{if } \Phi_i = 0 \\ \frac{2}{\pi\alpha} \left[ 1 + \left(\frac{\Phi_i}{\alpha}\right)^2 \right]^{-1} & \text{if } 0 < \Phi_i \leq \alpha \end{cases} \quad (32)$$

The regularized Heaviside function and Dirac delta function of Case 3 introduced by Berthelsen (2002) and Moog (2000) are defined as follows, respectively.

$$H_r(\Phi_i) = \begin{cases} 0 & \text{if } \Phi_i = 0 \\ \frac{1}{2} \left[ 1 + \frac{\Phi_i}{\alpha} + \frac{1}{\pi} \sin\left(\frac{\pi\Phi_i}{\alpha}\right) \right] & \text{if } 0 < \Phi_i \leq \alpha \end{cases} \quad (33)$$

$$\delta_r(\Phi_i) = \begin{cases} \frac{1}{\alpha} & \text{if } \Phi_i = 0 \\ \frac{\alpha}{2} \left[ 1 + \cos\left(\frac{\pi\Phi_i}{\alpha}\right) \right] & \text{if } 0 < \Phi_i \leq \alpha \end{cases} \quad (34)$$

The regularized Heaviside function and Dirac delta function of Case 4 introduced by Belytschko *et al.* (2003) are defined as follows, respectively.

$$H_r(\Phi_i) = \begin{cases} \frac{1}{2} & \text{if } \Phi_i = 0 \\ \frac{1}{2} \left[ 1 + \sin\left(\frac{\pi\Phi_i}{2\alpha}\right) \right] & \text{if } 0 < \Phi_i \leq \alpha \end{cases} \quad (35)$$

$$\delta_r(\Phi_i) = \begin{cases} \frac{\pi}{4\alpha} & \text{if } \Phi_i = 0 \\ \frac{\pi}{4\alpha} \cos\left(\frac{\pi\Phi_i}{\alpha}\right) & \text{if } 0 < \Phi_i \leq \alpha \end{cases} \quad (36)$$

The first polynomial regularized Heaviside function and Dirac delta function of Case 5 introduced in this study are defined as follows, respectively.

$$H_r(\Phi_i) = \begin{cases} \frac{1}{2} & \text{if } \Phi_i = 0 \\ \frac{1}{2} \left[ 1 + \left(\frac{\Phi_i}{\alpha}\right) \right] & \text{if } 0 < \Phi_i \leq \alpha \end{cases} \quad (37)$$

$$\delta_r(\Phi_i) = \begin{cases} 0 & \text{if } \Phi_i = 0 \\ \frac{1}{2\alpha} & \text{if } 0 < \Phi_i \leq \alpha \end{cases} \quad (38)$$

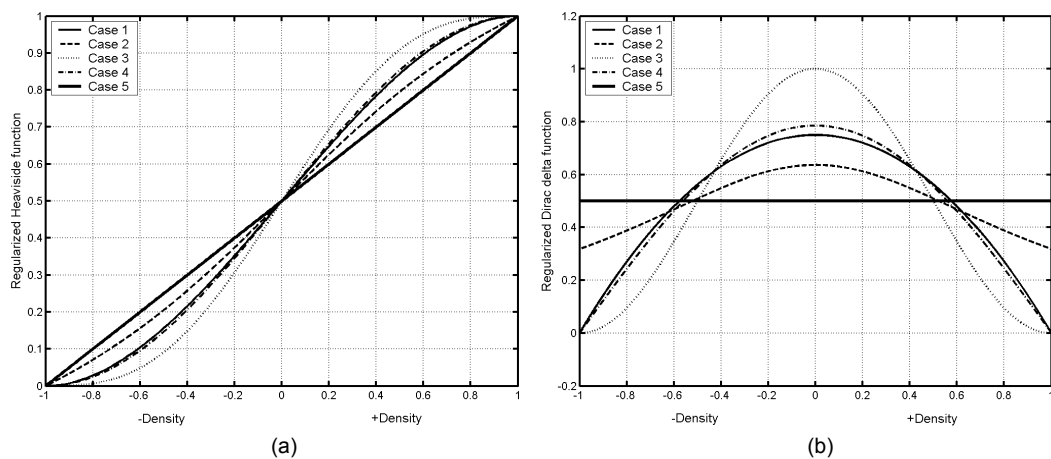


Fig. 10 Curves of regularized Heaviside function and Dirac delta function of Case 1~5: (a) Regularized Heaviside function (b) Regularized Dirac delta function

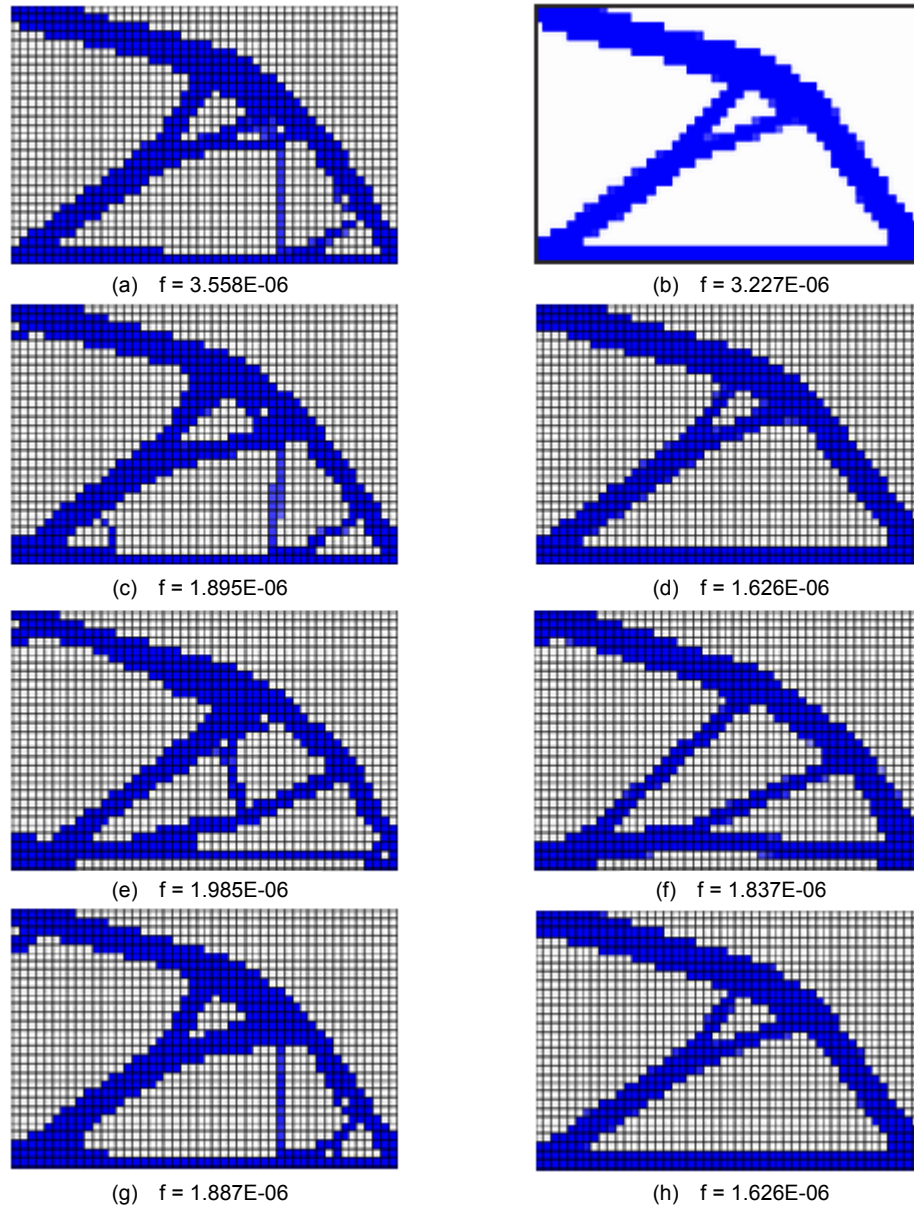


Fig. 11 Optimal density distributions of Fig. 7 (a): (a), (b)-Case 2 (c), (d)-Case 3 (e), (f)-Case 4 (g), (h)-Case 5 (a), (c), (e), (g)-regularized SIMP (b), (d), (f), (h)-Filtered and Regularized SIMP

The curves of the regularized Heaviside function and Dirac delta function of Cases 1~5 are shown in Fig. 10. The optimal structures by SIMP using regularization in Cases 2~5 are shown in Figs. 11 and 12. As can be seen, the use of a regularized Heaviside function for couple-signals results in improved optimal solutions with the best minimums of converged objective function values and numerical stabilities. In this study, optimality criteria method was used for updating

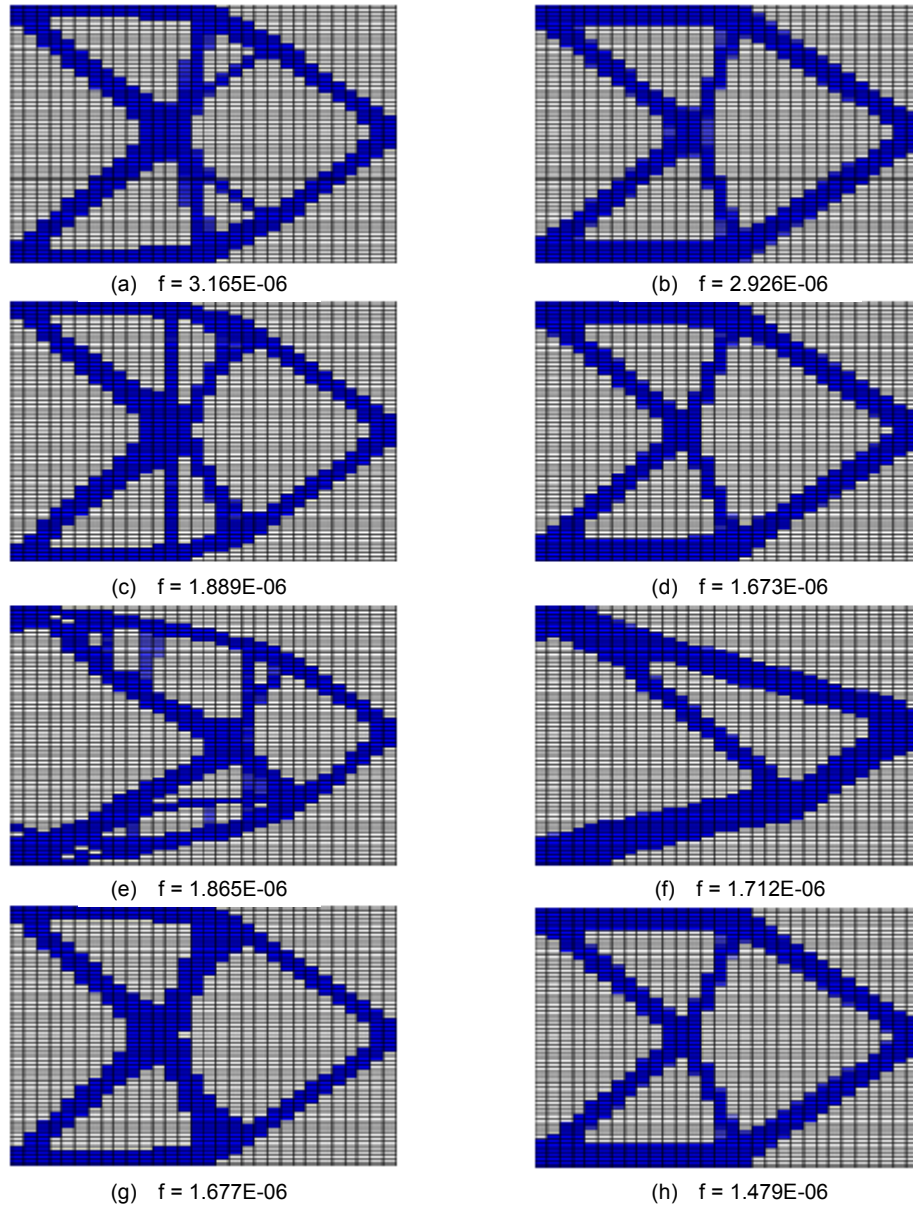


Fig. 12 Optimal density distributions of Fig.7 (b): (a), (b)-Case 2 (c), (d)-Case 3 (e), (f)-Case 4 (g), (h)-Case 5 (a), (c), (e), (g)-regularized SIMP (b), (d), (f), (h)-Filtered and Regularized SIMP

design variables. As can be seen, the optimality criteria for general application were found to be satisfactory for problems with few active constraints or with small numbers of design variables. For problems with large numbers of behavior constraints and design variables, the method would appear to follow a subset of active constraints that can result in a heavier design (Patnaik *et al.* 2005)

## 7. Conclusions

In this study, an improved approach based on regularization with couple-signals was proposed for a two-phase material topology optimization of the SIMP approach. The key point of this study is to use a regularized Heaviside function in optimization procedures for the SIMP, i.e., for a structural analysis, a sensitivity analysis, and an optimality criteria analysis. Basically, the Heaviside function uses a signal which determines if an element material exists or not. In the SIMP formulation, a material matrix also includes such an indication. In order to produce well-posed material topology optimization solutions and avoid numerical instabilities in design solutions, the SIMP approach with couple-signals, which combine design variable values with a regularized Heaviside function, is proposed instead of using filtering in SIMP.

Preliminarily, the regularized SIMP method has the same purpose as a sensitivity filtering method. The proposed approach has one similarity compared with the method introduced by Belytschko *et al.* (2003), which used an implicit function as a design variable to describe the topology of structures. The similarity is that both methods regularize the Heaviside function to achieve 0-1 solutions. However, the method employed by Belytschko *et al.* used nodal values as the design variable (to be precise, a nodal-based design), and projects those values onto the element domain. Therefore, the convergence rate may be very slow. Here, the proposed method seeks improved solutions in the field of the conventional SIMP formulation, i.e., an element-based design and offers direct control over material stiffness terms.

Because the material stiffness terms are multiplied by a regularized Heaviside function, each element loses stiffness during the optimization iterations. Therefore, differences of the relative stiffness and displacements naturally decrease continuously. The numerical phenomenon gives rise to improved 0-1 convergence solutions. The regularization formulation of the objective function such as Eq. (4) is not only suitable for Eq. (6), but is also suitable for other regularized Heaviside functions. Usable regularized Heaviside functions which have been introduced in other research literatures and optimal results for them have been shown in Section 6.2.

The new method, one regularized Heaviside function is another thing to be topologically optimized as several alternatives. The use of the regularized Heaviside function provides the best solution with respect to the converged objective function such as stiffness.

## Acknowledgements

This research was supported by a grant (code# 2013R1A1A2057502 & 2014R1A1A3A04051296) from the National Research Foundation of Korea (NRF) funded by the Korea government.

## References

- Belytschko, T., Xiao, S.P. and Parimi, C. (2003), "Topology optimization with implicit functions and regularization", *Int. J. Numer. Meth. Eng.*, **57**, 1177-1196.
- Bendsøe, M.P. (1989), "Optimal shape design as a material distribution problem", *Struct. Optim.*, **1**, 193-202.
- Bendsøe, M.P. and Haber, R. (1993), "The Michell layout problem as a low volume fraction limit of the

- homogenization method for topology design: an asymptotic study”, *Struct. Optim.*, **6**, 263-267.
- Bendsøe, M.P. and Sigmund, O. (1999), “Material Interpolations in topology optimization”, *Arch. Appl. Mech.*, **69**, 635-654.
- Bendsøe, M.P. and Kikuchi, N. (1988), “Generating optimal topologies in structural design using a homogenization method”, *Comput. Meth. Appl. Mech. Eng.*, **71**, 197-224.
- Berthelsen, P.A. (2002), “A short Introduction to the Level Set Method and Incompressible Two-Phase Flow, A Computational Approach”, Technical Report, Department of Applied Mechanics, Thermodynamics and Fluid Dynamics, Norway University of Science and Technology.
- Bourdin, B. (2001), “Filters in topology optimization”, *Int. J. Numer. Meth. Eng.*, **50**, 2143-2158.
- Diaz, A.R. and Bendsøe, M.P. (1992), “Shape optimization of structures for multiple loading conditions using a homogenization method”, *Struct. Optim.*, **4**, 17-22.
- Diaz, R.I. and Sigmund, O. (1995), “Checkerboards patterns in layout optimization”, *Struct. Optim.*, **10**, 40-45.
- Eschenauer, H.A., Kobelev, V.V. and Schmacher, A. (1994), “Bubble method for topology and shape optimization of structures”, *Struct. Optim.*, **8**, 42-51.
- Fujii, D., Chen, B.C. and Kikuchi, N. (2001), “Composite material design of two-dimensional structures using the homogenization design method”, *Int. J. Numer. Meth. Eng.*, **50**, 2031-2051.
- Guest, J.K., Prevost, J.H. and Belytschko, T. (2004), “Achieving minimum length scale in topology optimization using nodal design variables and projection function”, *Int. J. Numer. Meth. Eng.*, **61**, 238-254.
- Hafka, R.T. and Guerdal, Z. (1992), *Elements of Structural Optimization*, Third Revised and Expanded Edition, Kluwer Academic Publishers.
- Haug, E.J., Choi, K.K. and Komkov, V. (1986), *Design Sensitivity Analysis of Structural Systems*, Academic Press Orlando, New York.
- Kawamoto, A., Matsumori, T., Yamasaki, S., Nomura, T., Kondoh, T. and Nishiwaki, S. (2011), “Heaviside projection based topology optimization by a PDE filtered scalar function”, *Struct. Multidisc. Optim.*, **44**(1), 19-24.
- Kohn, R.V. and Strang, G. (1986), “Optimal design and relaxation of variational problems”, *Commun. Pure Appl. Math.*, **39**, 113-137.
- Lee, D.K., Lee, J.H., Lee, K.H. and Ahn, N.S. (2014a), “Evaluating topological optimized layout of building structures by using nodal material density based bilinear interpolation”, *J. Asian Arch. Build. Eng.*, **13**, 421-428.
- Lee, D.K., Shin, S.M., Lee, J.H. and Lee, K.H. (2015a), “Layout evaluation of building outrigger truss by using material topology optimization”, *Steel Compos. Struct.*, **19**(2), 263-275.
- Lee, D.K. and Shin, S.M. (2015b), “Extended-finite element method as analysis model for Gauss point density topology optimization method”, *J. Mech. Sci. Tech.*, **29**(4), 1341-1348.
- Lee, D.K. and Shin, S.M. (2015c), “Optimising node density-based structural material topology using eigenvalue of thin steel and concrete plates”, *Mater. Res. Innov.*, **19**(S5), 1241-1245.
- Moog, M. (2000), “Level set methods for hele-shaw flow”, Ph.D Thesis, Department of Mathematics, University of Kaiserslautern.
- Osher, S. and Fedkiw, R. (2001), “Level set methods: An overview and some recent results”, *J. Comput. Phys.*, **169**, 475-502.
- Osher, S. and Paragios, N. (2003), *Geometric Level Set Methods in Imaging, Vision, and Graphics*, Springer Verlag.
- Patnaik, S.N., Guptill, J.D. and Berke, L. (2005), “Merits and limitations of optimality criteria method for structural optimization”, *Numer. Meth. Eng.*, **38**(18), 3087-3120.
- Rozvany, G.I.N. (2001), “Aims, scope, methods, history and unified terminology of computer aided topology optimization in structural mechanics”, *Struct. Multidisc. Optim.*, **21**, 90-108.
- Rozvany, G.I.N., Zhou, M. and Birker, T. (1992), “Generalized shape optimization without homogenization”, *Struct. Optim.*, **4**, 250-252.
- Sigmund, O. (1994), “Design of material structures using topology optimization”, DCAMM Special Report

- No. 569, Technical University of Denmark.
- Sigmund, O. and Petersson, J. (1998), "Numerical instabilities in topology optimization: a survey on procedures dealing with checkerboards, mesh-dependencies and local minima", *Struct. Optim.*, **16**(1), 68-75.
- Sigmund, O. (2001), "A 99 topology optimization code written in Matlab", *Struct. Multidisc. Optim.*, **21**, 120-127.
- Wang, M.Y., Wang, X. M. and Guo, D.M. (2003), "A level set method for structural topology optimization", *Comput. Meth. Appl. Mech. Eng.*, **192**(1-2), 227-246.
- Wang, X.M., Wang, M.Y. and Guo, D.M. (2004), "Structural shape and topology optimization in a level-set based framework of region representation", *Struct. Multidisc. Optim.*, **27**, 1-19.
- Zhu, B., Zhang, X. and Fatikow, S. (2015), "Structural topology and shape optimization using a level set method with distance-suppression scheme", *Comput. Meth. Appl. Mech. Eng.*, **283**, 1241-1239.
- Zienkiewicz, O.C. and Campbell, J.S. (1973), *Shape Optimization and Sequential Linear Programming, Optimum Structural Design*, Eds. Gallagher, R.H. and Zienkiewicz, O.C., 109-126.